

Growth and magnetism of Co nanometer-scale dots squarely arranged on a Cu(001)- $c(2\times 2)$ N surface

F. Komori,* K. D. Lee,*[†] K. Nakatsuji, T. Iimori, and Y. Q. Cai*[‡]

Institute for Solid State Physics, University of Tokyo, Kashiwa-shi, Chiba 277-8581, Japan

(Received 5 August 2000; revised manuscript received 27 November 2000; published 14 May 2001)

We have studied the growth and magnetism of two-dimensionally coupled nanometer-scale Co dots which are squarely arranged on a Cu(001)- $c(2\times 2)$ N surface. The morphology was analyzed by scanning tunneling microscopy, and the magnetization was studied using the magneto-optical Kerr effect. Well-ordered arrays of two monolayer (ML) thick Co dots interconnected by narrow 1 ML thick Co films can be grown by adjusting the deposited amount of Co. Here we used selective growth of Co at the clean Cu area of the surface, which consists of 5×5 nm² N-adsorbed $c(2\times 2)$ patches separated by clean Cu lines of a few nm in width. The observed ferromagnetism in these arrays is considered to be mediated by narrow monolayer thick Co films on clean Cu lines. When the average thickness of Co exceeds 1.5 ML, 2 ML thick Co dots are connected with each other, and 1 ML Co films grow on the $c(2\times 2)$ N patches. For Co films with an average thickness between 1.8 ML and 2.1 ML, the magnetization is almost constant between 150 K and 370 K, and increases with decreasing temperature from 150 K. This result suggests that polarization is induced in the 1 ML Co film on $c(2\times 2)$ N patches below 150 K.

DOI: 10.1103/PhysRevB.63.214420

PACS number(s): 75.70.Ak

I. INTRODUCTION

Thin ferromagnetic transition metals on normal metals have been intensively studied for an understanding of low-dimensional magnetism. In these systems, magnetic long-range order is established by increasing the nominal thickness of the transition metals within a few atomic monolayers (ML's). For example, in Fe(110)/W(110),¹ detailed measurements of the surface morphology and the magnetic transition revealed that the ordering process is a two-dimensional magnetic percolation. A similar mechanism for long-range order was proposed for Co/Cu(001).² For further study of the magnetic interaction in nanometer-scale structures, however, these random networks of magnetic islands are not suitable for macroscopic measurements of spatially averaged quantities because of inhomogeneities in the lateral size and the thickness of the magnetic islands. In order to study the size and shape dependence of the magnetic interaction, controlled fabrication of ordered nanometer-scale structures is required. Recently, equally spaced monoatomic steps and self-organized strain-relief patterns on metal surfaces have been used as templates for the growth of one- and two-dimensional nanostructures. In particular, the magnetic properties of Fe/Cu(111),³ Fe/W(110),⁴ and Co/Au(111) (Ref. 5) have been studied.

In the present article, we report on the growth and the magnetism of a square array of 2 ML thick Co dots on a nitrogen-modified Cu(001) surface. We used an ordered structure reported by Leibsle *et al.*⁶ as the template. They showed that $c(2\times 2)$ N square patches of 5 nm \times 5 nm in size can be arranged squarely on a clean Cu(001) surface with a separation of a few nm by adjusting the amount of N. It was considered⁷ that this surface is formed to relieve the surface strain caused by the lattice mismatch between Cu and the $c(2\times 2)$ N patches.

The growth of magnetic⁸⁻¹¹ and nonmagnetic¹² metals has

been studied on this surface previously. These metals grow selectively on the clean Cu part of the surface at the early stage of the deposition at room temperature (RT), although the details of the growth are dependent on both the metal species and the morphology of the surface. In the case of Ni,⁹ 1 or 2 ML thick isolated Ni islands grow selectively at the crossings of the clean Cu lines. On the other hand, in the case of Co, all the Cu lines are covered with monolayer Co at first,^{10,11} and then bilayer Co islands are squarely arranged at the crossings and are interconnected with monolayer Co strips.

We have studied the growth of Co at RT using scanning tunneling microscopy (STM), and the magnetic properties using the surface magneto-optical Kerr effect (SMOKE). Among the magnetic transition metals on Cu(001) surfaces, Co has the following advantages: The growth of Co on clean Cu(001) is known to be simply epitaxial at least in the first several monolayers. Moreover, the magnetic properties have been extensively studied. For example, the Curie temperature of 2 ML thick Co on clean Cu(001) is higher than RT, and monolayer Co has no magnetization down to 50 K.¹³ These are useful for a discussion of the experimental results of the present system. On the basis of the observed morphology of the squarely arranged dots, we discuss the magnetic properties, especially the roles of monolayer Co films on the surface. Preliminary results of the magnetic properties have been published in Ref. 14.

II. EXPERIMENT

A. STM observation

The growth of Co dots arrays was studied in an ultrahigh vacuum (UHV) using a scanning tunneling microscope (Omicron, microSTM head) with a tungsten tip. The UHV system consisted of a preparation chamber and an STM chamber separated by a gate valve. The latter was equipped

with a four-grid low-energy electron diffraction (LEED) optics (OCI, BLD600). The base pressure of both chambers was better than 1×10^{-10} Torr. A clean surface of Cu(001) was obtained by repeating Ar ion sputtering (500 eV) and annealing at 970 K in the preparation chamber. Then the cleaned sample was transferred to the STM chamber. We confirmed the cleanness of the surface by Auger electron spectroscopy (AES), the structural order by a sharp 1×1 LEED pattern, and surface morphology by STM.

To prepare the nitrogen-modified surface, a clean Cu(001) surface was bombarded by nitrogen ions of 500 eV, followed by annealing at 600 K for typically 5 min in the preparation chamber. We monitored the ion current at the sample during the N ion bombardment to adjust the amount of implanted nitrogen into the substrate. The regular arrangement of $c(2 \times 2)$ N square patches was confirmed by STM. We also observed the correlation between the order of the arrangement and a satellite structure around the integral LEED spots.¹⁴

In the STM chamber, Co deposition was made from an alumina crucible, around which a resistively heated tantalum wire was wound. We kept the substrate temperature at RT to reduce intermixing of the deposited Co and the Cu substrate.¹⁵ The deposition rate was 0.1 ML/min as monitored by a quartz microbalance. The pressure during the deposition was less than 5×10^{-10} Torr. The average thickness of Co was calibrated by estimating the amount of Co on the surface from the STM images. At the same time, we measured the intensity ratio of the Co *LMM*(716 eV) Auger line to Cu *LMM*(920 eV) line as a function of the average thickness of Co on the surface.

STM images were taken with a constant-current mode at RT. The typical tunneling current was 1 nA, and the sample bias voltage was 1 V. No correction was made to any distortion of the images in the present paper.

B. Magnetization measurements

The magnetic properties were measured by SMOKE in another UHV system consisting of a measurement chamber with a LEED optics (OCI, BLD600) and a preparation chamber. The base pressure of the chambers was better than 2×10^{-10} Torr. The SMOKE signal was measured *in situ* in longitudinal and polar configurations with *s*-polarized light from a He-Ne laser. Two pairs of Helmholtz coils for longitudinal and polar configurations were placed in the chamber for this purpose. The fluence of the light was 5 mW/cm². A lock-in technique was employed by modulating the incident light with a photoelastic modulator. During the SMOKE measurement, the sample temperature could be controlled between 90 K and 450 K. The temperature during the measurement was monitored by a thermocouple attached to the side of the Cu crystal.

The Co nanostructures were prepared in the same way as for the STM experiments except that the Co source was a resistively heated W wire wrapped with a Co wire. To ensure the substrate morphology with a regular arrangement of $c(2 \times 2)$ N square patches, we utilized LEED patterns showing the satellites around integer-ordered spots.¹⁴ The thick-

ness of Co was monitored by a quartz microbalance, which was calibrated by the measured Co/Cu Auger ratio. Here we use the relation between the Co/Cu Auger ratio and the averaged Co thickness calibrated by the STM observation. To confirm the calibration, we measured the Curie temperature (T_c) of Co films grown on a clean Cu(001) surface as a function of the calibrated thickness. As in the literature,¹³ we experimentally defined T_c as the temperature at which the remanence magnetization detected by SMOKE vanishes. We found that the values of T_c were consistent with those reported in this literature. The accuracy of the obtained Co thickness is about 15% because of the uncertainty in the measured Auger ratio.

III. RESULTS AND DISCUSSION

A. Growth of Co dot array

Figure 1 shows typical STM images of a N-adsorbed Cu(001) surface for two different amounts of N. By adjusting the amount of N, we could obtain a regular and square arrangement of $c(2 \times 2)$ N square patches as in Fig. 1(a). With increasing amount of adsorbed nitrogen, the clean Cu(001) mesh lines separating the $c(2 \times 2)$ N patches become narrower, and there appear trenches with monoatomic layer depth as shown in Fig. 1(b). These trenches are formed to relieve the surface strain just as the grids of clean Cu lines. The small areas with square arrays of $c(2 \times 2)$ N patches are separated by trenches or steps on the surface. We note that the density of the steps increases after formation of the $c(2 \times 2)$ N patches. These features are consistent with a previous report.⁷

The morphology of the N-adsorbed surface is dependent on annealing conditions. We found that the width of the clean Cu lines becomes anisotropic by increasing the annealing temperature to 630 K while keeping the other conditions unchanged. Figure 1(c) is an STM image of such a surface. In one small domain, the width of bright Cu lines along the [100] direction is larger than that along the [010] direction, whereas it is the opposite in the other domain. This surface could be used as a possible template for the growth of one-dimensional magnets¹¹ although it seems difficult to prepare a single-domain surface for macroscopic measurements.

The growth of Co on the surface with a regular arrangement of $c(2 \times 2)$ N patches is shown in Fig. 2. At the initial stage of the deposition, single atomic layer Co grows selectively on the clean Cu lines as in Fig. 2(a) when the width of the line is larger than 1 nm. With increasing amount of deposited Co on the surface, monolayer continuous Co lines are formed, and the second atomic layer grows selectively at the crossings of the Cu lines as in Fig. 2(b). Further deposition of Co results in a square arrangement of the bilayer Co dots interconnected with monolayer strips as shown in Fig. 2(c). A schematic model for this film is given in Fig. 2(e). At this stage, a part of the $c(2 \times 2)$ N patches are covered with monolayer Co. These observations are consistent with previous reports.^{10,11} When the average thickness of Co is larger than 1.8 ML, most of the bilayer islands are connected with one another. Furthermore, the third atomic layer is formed not always at the crossings of the clean Cu lines. At the same

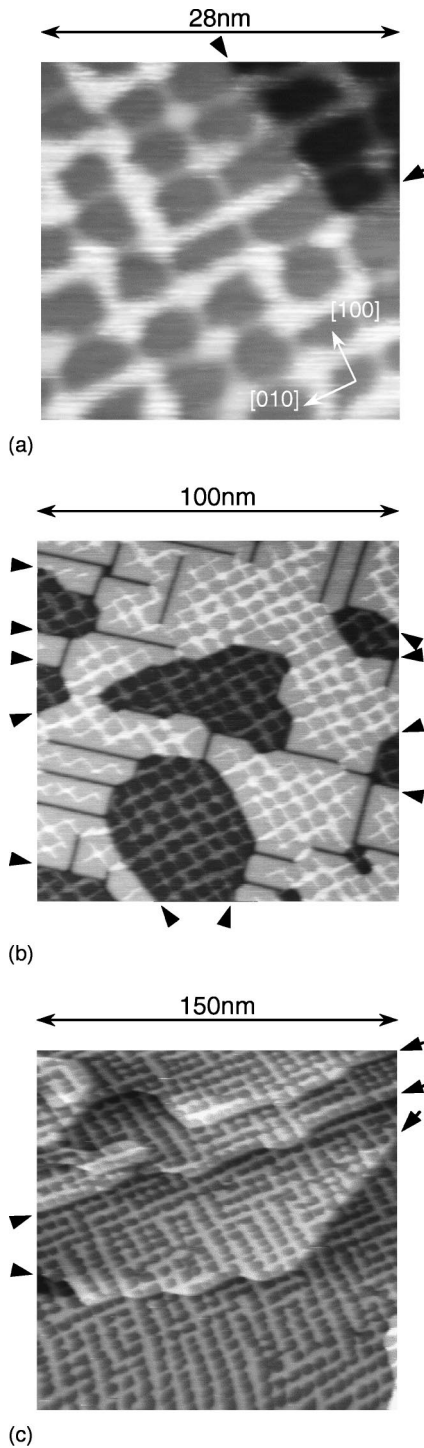


FIG. 1. STM images of nitrogen-adsorbed surfaces prepared with three different conditions. Arrows indicate the positions of steps with the monoatomic height. (a) The surface with squarely arranged $c(2 \times 2)N$ patches (dark area) separated by clean Cu surface (bright grids). The nitrogen coverage of the surface is 0.3 ML on average. (b) The surface with square patches and monoatomic height trenches. The density of Cu lines with subnanometer widths is higher than that shown in (a). The nitrogen coverage of the surface is 0.4 ML on average. (c) The surface with anisotropic Cu lines. The annealing temperature is higher than that in (a) and (b). The nitrogen coverage of the surface is 0.2 ML on average.

time, most of the N-adsorbed patches are covered with 1 ML Co film at first, and then the second ML is formed on it with an increased average thickness of Co. Consequently, the square arrangement of Co dots becomes disordered. An STM image of such a surface is shown in Fig. 2(d) for a film with 1.9 ML Co on average. A schematic drawing for the morphology of this film is given in Fig. 2(f). Figure 3 shows an STM image of $200 \text{ nm} \times 200 \text{ nm}$ for 1.3 ML Co. We observe a homogeneous arrangement of the Co dots and distribution of monoatomic steps on the substrate.

For all surfaces with an average Co coverage of up to 2 ML, the LEED patterns were always $c(2 \times 2)$ although the sharpness of the spots became worse with increasing Co thickness. This indicates that the $c(2 \times 2)N$ structure is stable against Co deposition of a few ML thick, and that Co growth is epitaxial with the substrate as in the case of Co grown on a clean Cu(001).

We note that there are at least three kinds of Co thin structures on the surface: 1 ML Co on clean Cu lines, 1 ML Co on $c(2 \times 2)N$ patches, and 2 ML Co dots. We will discuss the result of the magnetization measurements by considering the magnetic properties of these components.

B. Magnetic properties

Figure 4(a) shows the evolution of hysteresis loops measured by longitudinal SMOKE at 95 K as the average Co thickness is increased. In Fig. 4(b), the magnitude of remanent magnetization is plotted as a function of the Co thickness. A magnetic field was applied in the plane along the $[110]$ direction which is the easy axis of magnetization for ultrathin Co films grown on a clean Cu(001) surface.¹³ Finite remanence begins to appear in the hysteresis loops taken for the 1.3 ML thick film. As the thickness is increased, the magnitudes of the magnetization and the coercivity increase. Beyond 2.2 ML the loop exhibits a rectangular shape, implying that the $[110]$ direction is the easy axis of magnetization. However, below 2 ML, the loops deviate significantly from this easy axis behavior. The shapes of the hysteresis loops were almost independent of the sweep rate between 40 Oe/sec and 2.5 Oe/sec. We could not detect any polar SMOKE signal in the Co thickness range we investigated.

Figure 5 shows the temperature dependence of hysteresis loops for the Co thickness of 1.3 ML (a), 1.6 ML (b), and 1.8 ML (c). We define here T_r as the temperature at which the remanence vanishes completely. The value of T_r lies around 160 K for 1.3 ML and 260 K for 1.6 ML. The transition was reversible because the same ferromagnetic Kerr loops could be reproduced after cooling the sample again. For 1.8 ML, the remanence persists up to 370 K, which indicates that T_r is above that temperature. We did not try to measure the Kerr loops over 400 K because a significant intermixing of Co with Cu may change the magnetic properties.¹⁵ In Fig. 6, the remanent magnetization as a function of temperature is shown for 1.6 ML and 1.8 ML. The remanence increases below 150 K for the 1.8 ML Co film, in which the saturated magnetization also increases below this temperature. Similar increases of the magnetizations were observed for 1.9 ML and 2.1 ML.

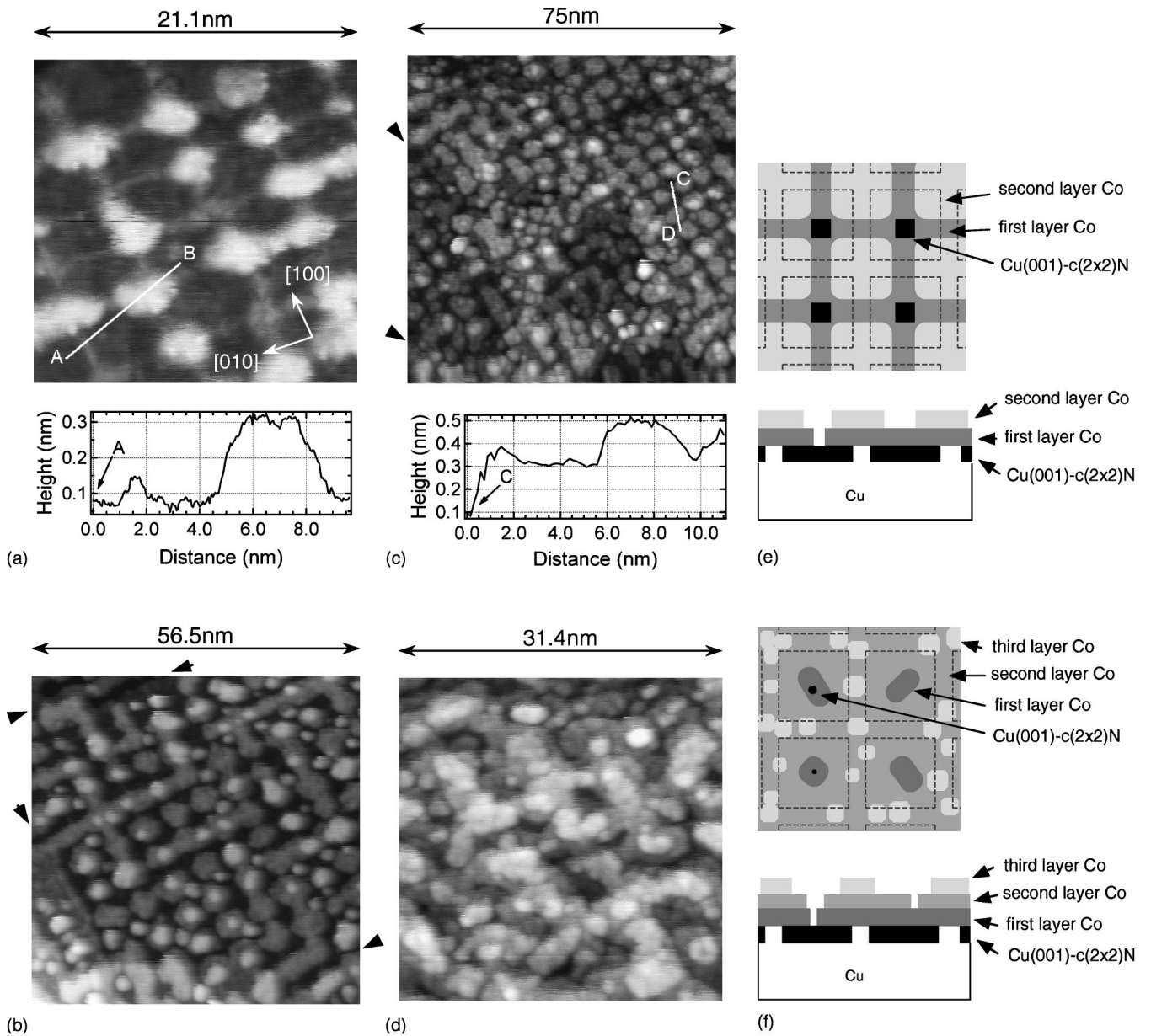


FIG. 2. STM images for Co grown on surfaces with squarely arranged $c(2 \times 2)N$ patches (a)–(d) and the gray-scale schematic models (e) and (f) for the surfaces (c) and (d), respectively. The average thicknesses of Co are (a) 0.2 ML, (b) 0.8 ML, (c), (e) 1.4 ML, and (d), (f) 1.9 ML. Arrows indicate the positions of steps, and dotted lines in (e) and (f) the boundaries between the $c(2 \times 2)N$ patches and the clean Cu(001) surfaces.

For further discussion on our magnetic data we point out that remanence is neither a necessary nor a sufficient condition for ferromagnetism—that is, a long-range order characterized by spontaneous magnetization. In the case of soft-magnetic materials ferromagnetic order is not necessarily accompanied by a remanence ($T_r < T_c$ in the present context), whereas “micromagnetic” effects such as superparamagnetic blocking may yield a remanence in the systems which are, in a strict sense, nonferromagnetic ($T_r > T_c$).

In Fig. 7, the change of T_r is plotted with increasing Co thickness. The uncertainty in the Co thickness is shown at the point for 1.3 ML. The arrows pointing up and down for

1.2 ML and 1.9 ML mean that the corresponding T_r is below 100 K and above 400 K, respectively. For comparison, the T_c for ultrathin Co films grown on a clean Cu(001) surface reported by Schneider *et al.*¹³ and Bovensiepen *et al.*¹⁶ are reproduced as dashed and solid lines, respectively. We note that the definition of T_c for Co films on clean Cu(001) is experimentally the same as that of T_r for the present system.

The measured T_r for Co on Cu(001)- $c(2 \times 2)N$ is found to be higher than T_c for Co/Cu(001) with the same nominal thickness within our experimental accuracy. This is ascribed to the difference in the growth morphology of Co islands. On the Cu(001)- $c(2 \times 2)N$ surface, bilayer islands are con-

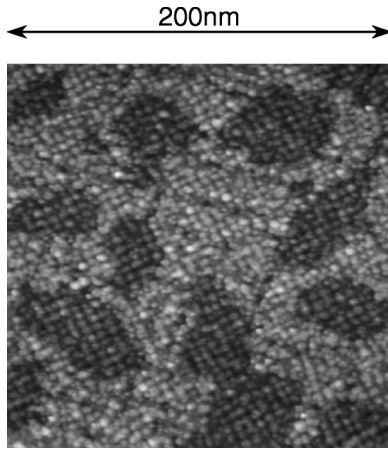


FIG. 3. STM image of square lattice of bilayer Co dots over a wide area of Cu(001)- $c(2 \times 2)N$ surface with monoatomic height steps. Average Co thickness is 1.3 ML.

nected with one another and a third layer is formed with an increased average thickness of Co. Even after the growth of the third layer, there remain small areas of bare $c(2 \times 2)N$ surface at the center of the patches. On the other hand, on clean Cu(001) surfaces, Co films are known to grow as bilayer islands just before coalescence.¹⁷ Consequently, the percolative transition² to a long-range two-dimensional (2D) ferromagnetic state for bilayer Co dots on Cu(001)- $c(2 \times 2)N$ should occur even if the average thickness of Co is smaller than that of the Co film on clean Cu(001). The increase of the effective thickness due to the confined growth of Co islands on Cu(001)- $c(2 \times 2)N$ causes a higher T_r than T_c of Co on clean Cu(001).

For an average thickness of less than 1.4 ML, the bilayer Co dots are separated from one another although they are connected with 1 ML Co short strips. These 2 ML thick dots do not seem to interact directly via exchange interaction because the monolayer Co on a clean Cu(001) surface is not ferromagnetic down to 50 K.^{13,16} Thus, the array of the isolated bilayer Co dots is expected to exhibit a superparamagnetic behavior below the Curie temperature for 2 ML Co films on a clean Cu(001) surface. Each Co dot has a spontaneous magnetization, and its direction is thermally fluctuating. The magnetization curves characteristic of superparamagnetism are really observed at 1.3 ML above 160 K and at 1.6 ML above 260 K [Figs. 5(a) and 5(b)] with no remanence but finite magnetization in the magnetic field. On the other hand, the presence of remanence below 150 K suggests a long-range 2D ferromagnetic transition of the array of Co dots. It is possible that each bilayer Co island has a sufficient magnetic moment to polarize nearby Co atoms in the 1 ML thick strips. We propose that the long-range ferromagnetic transition occurs through interaction among the bilayer Co islands mediated by the induced polarization in short Co strips.

The onset of ferromagnetic order in two-dimensional networks of the type considered in the present work has been theoretically investigated using renormalization group analysis of the Ising model.²⁰ Long-range ferromagnetic order was found to be established among superparamagnetic nanodots

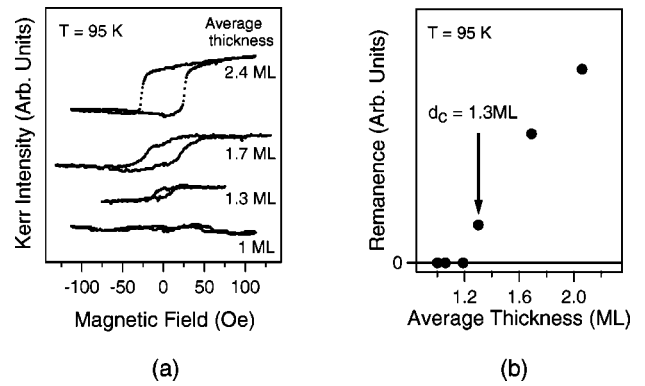


FIG. 4. (a) Hysteresis loops of the magnetization along [110] as a function of average Co thickness at 95 K. (b) Remanence magnetization at 95 K as a function of average Co thickness. An arrow at d_c is the critical Co thickness for the appearance of the remanence.

below T_c through interdot magnetic coupling. In our films, superparamagnetism of each bilayer Co dot is ensured by interaction among the Co atoms in the dot, whereas interdot coupling is realized by monolayer Co regions.

Below 1.2 ML, the magnetic interaction mediated by short Co strips becomes too weak to induce ferromagnetism above 95 K although each Co dot may behave as a superparamagnet. For these films, we have no evidence of superparamagnetism, which should be examined by using higher magnetic fields as demonstrated for Co dots on a Au(111) surface.⁵ The maximum magnetic field of 200 Oe in the present study is insufficient to saturate all the superparamagnetic moments at the Co dots even at 95 K.

Another possible explanation of the hysteresis loop at 1.3 ML below 150 K is the blocking of superparamagnets. The blocking generally occurs with decreasing temperature when the relaxation time of superparamagnet τ becomes longer than the measuring time. We observed that the hysteresis curve is independent of the sweep rate if it is faster than 2.5 Oe/sec. This experimentally excludes the blocking as long as τ is shorter than a few minutes. The value of τ at T for a particle with a volume V can be estimated from the Néel equation¹⁸ given by

$$\frac{1}{\tau} = f_0 \exp \frac{-KV}{k_B T}, \quad (3.1)$$

where K is the absolute value of the intrinsic magnetic anisotropy constant and f_0 the characteristic frequency of the magnetic system of the order of 10^9 sec. Using this equation with the known isotropic constant of Co film on clean Cu(001), $K = 10^6$ erg/cm³ (Ref. 19), and $T = 150$ K, we obtain $\tau = 10^{-19}$ sec for a bilayer island with 5 nm \times 5 nm in lateral size. This is much shorter than the measuring time.

We observed increasing magnetization below 150 K for Co films with thicknesses between 1.8 and 2.1 ML (see Fig. 6). In these films, 2 or 3 ML thick Co is well connected and T_r is higher than 370 K. Then, the magnetization due to the 2 or 3 ML thick Co film on these surfaces should be saturated below 150 K, which is much less than their transition

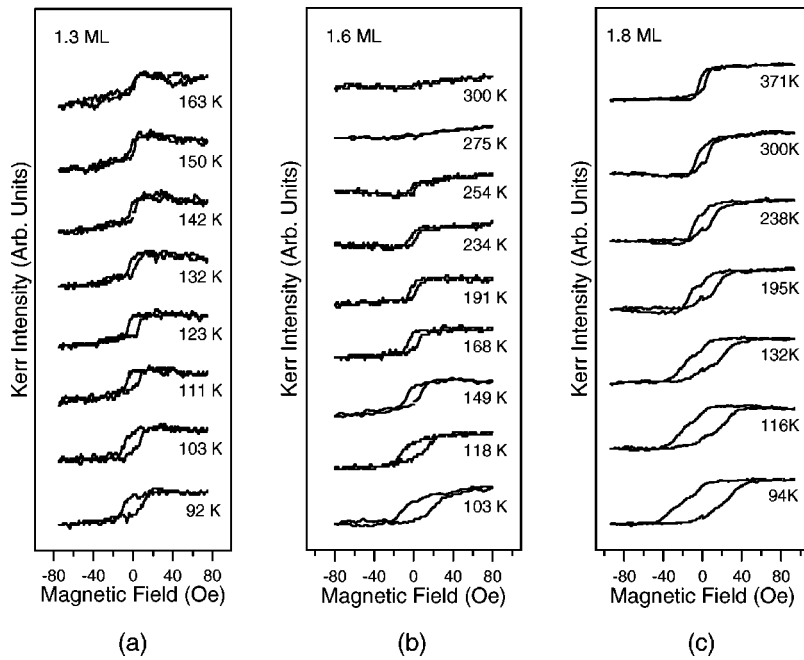


FIG. 5. Hysteresis loops as a function of temperature for three samples. The average thicknesses of Co are (a) 1.3 ML, (b) 1.6 ML, and (c) 1.8 ML.

temperature to the long-range ferromagnetic state. Thus a possible origin of the increasing magnetization with decreasing temperature is the polarization of the magnetic moments at the areas of monolayer Co on $c(2 \times 2)N$ patches. We found such areas around connected 2 or 3 ML thick Co in the STM images for these films. Polarization at the monolayer area may be induced by the neighboring 2 or 3 ML thick Co.

For the 1.6 ML thick film, the magnetization due to the bilayer dots gradually increases with decreasing temperature from $T_r = 260$ K, and has no clear plateau. Thus, we could not experimentally separate the induced polarization at the monolayer area from the magnetization due to the bilayer dots. For the film with more than 2.2 ML thick Co, the area with monolayer Co becomes very small, and the magnetic properties become almost the same as the Co film on a clean Cu(001) surface.

We observed reduced remanence from the saturated mag-

netization for films with average thicknesses of less than 2.1 ML. This implies the possible change of the easy axis of magnetization. The fcc Co film on a clean Cu(001) surface has a fourfold easy axis of magnetization along $[110]$,¹³ which is governed by the magnetocrystalline anisotropy. In this context, the atomic arrangement within the Co dots is important. A recent study²¹ by surface-extended x-ray absorption fine structure revealed that the Fe atoms on Cu(001)- $c(2 \times 2)N$ are arranged in an fcc lattice with tetragonal distortion as in Fe/Cu(001) films. If Co grows in the same way, the magnetocrystalline anisotropy does not change whether Co is grown on Cu(001) or on Cu(001)- $c(2 \times 2)N$. The recovery of full remanence beyond 2.2 ML supports the fcc structure of Co.

In addition to magnetocrystalline anisotropy, shape anisotropy may also play an important role in determining the magnetoanisotropy energy. Since the Co strips on Cu(001)- $c(2 \times 2)N$ are along the $[100]$ and $[010]$ directions,

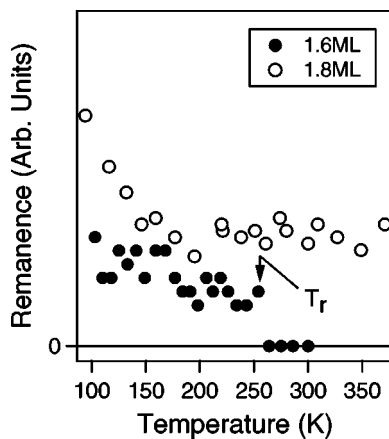


FIG. 6. Remanence magnetization as a function of temperature for samples with 1.6 ML (solid circles) and 1.8 ML (open circles) Co on average. The transition temperature T_r of 1.6 ML thick sample is indicated by an arrow.

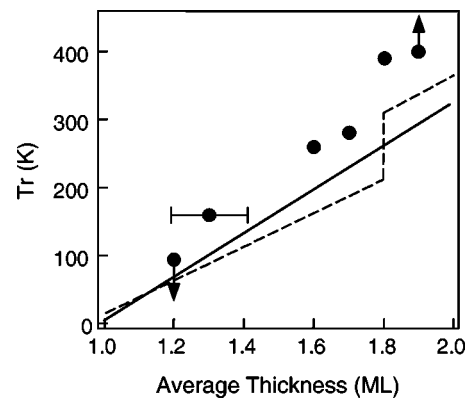


FIG. 7. The transition temperature T_r as a function of the average thickness of Co. Solid and dashed lines are the Curie temperature T_c for Co films on clean Cu substrates reproduced from Refs. 13 and 16, respectively.

it is plausible that the shape anisotropy favoring $[100]$ or $[010]$ directions as an easy axis of magnetization competes with the magnetocrystalline anisotropy. The measurement of Kerr loops along the $[100]$ direction, however, did not produce rectangular shapes. This suggests that the shape anisotropy posed by the arrangement of Co dots is not a dominant factor in determining the easy axis. Another possible source of magnetic anisotropy is the steps generated during the preparation of the substrate. The presence of steps on the substrate has a profound influence on the magnetic anisotropy.^{22,23} The step density on the substrate increases after the formation of regularly arranged square patches of $c(2 \times 2)N$ islands as shown in Fig. 3. Since the steps tend to run along both the $[110]$ and $[100]$ directions, they will give eightfold symmetry in the magnetic anisotropy. Therefore, three sources of anisotropy compete with one another, resulting in the complicated nature of the present system.

For Co grown on a clean Cu (001) surface, it was pointed out¹⁷ that the details of morphology and interface mixing between Co and Cu depend on the deposition rate and the substrate temperature. The intermixing weakens the magnetic interaction, especially in a few ML thick films. In the present case, the monolayer Co film directly grown on $c(2 \times 2)N$ patches is free from intermixing because the nitrogen-adsorbed structure is not broken by the Co deposition. In the above discussion, we proposed that induced polarization is present in this film. It is even possible that the monolayer Co film on the patches has spontaneous magnetization at low temperature. As for Co on clean Cu lines on the $c(2 \times 2)N$ surface, it is not known whether intermixing takes place similarly to Co on a clean Cu(001) surface. We do notice that the apparent height in the STM images is inhomogeneous on an isolated 1 ML Co dot grown at a crossing of the Cu lines. This result resembles evidence of intermixing on a clean Cu(001) surface.¹⁷ However, it is sometimes misleading to discuss the origin of the contrast only by STM

observations. Further studies of the structures both theoretically and experimentally are necessary to understand the nanoscale magnetism.

IV. CONCLUSION

Regular arrays of Co nanoscale dots were grown on a Cu(001)- $c(2 \times 2)N$ surface. At the initial stage of the deposition, Co selectively covers a clean Cu area on the surface consisting of squarely arranged $c(2 \times 2)N$ patches and clean Cu(001) grids of a few nm in width. When the amount of deposited Co is increased, the second ML of Co grows preferentially at the intersections of the Cu grids. The transition temperature to a long-range 2D ferromagnetic state increases with an increased average Co thickness, and is higher than that for a Co film directly deposited on a clean Cu(001) surface with the same average thickness. This is attributed to the confined growth of Co islands on Cu(001)- $c(2 \times 2)N$. Remanent magnetization is observed for the 1.3 ML film in which the bilayer Co dots have not been percolated. For films with an average thickness between 1.8 and 2.1 ML, the magnetization increases with decreasing temperature below 150 K, which is much smaller than the corresponding transition temperature to the long-range ferromagnetic state. We propose that the polarization is induced in monolayer Co films both on clean Cu lines and on $c(2 \times 2)N$ patches by the neighboring bilayer Co dots at low temperature and mediates the ferromagnetic interaction among the isolated bilayer Co dots in the 1.3 ML film.

ACKNOWLEDGMENTS

We would like to thank K. Tanaka, Y. Matsumoto, and K. Mukai for valuable discussions on the growth of the crystals, and K. Hattori and M. Yamada for their collaboration on the magnetization measurements at an early stage of the experiment.

*Also at CREST, Japan Science and Technology Corporation, Saitama, Japan.

[†]Present address: Innovation Center, LG Electronics Institute of Technology, 16 Woomyeon-dong, Seocho-gu, Seoul 137-724, Korea.

[‡]Present address: Taiwan Beamline Office at Spring-8, 1-1-1 Kouto, Mikazuki-cho, Sayo-gun, Hyogo 679-5198, Japan.

¹H.J. Elmers, J. Hauschild, H. Hoeche, U. Gradmann, H. Bethge, D. Heuer, and U. Koehler, *Phys. Rev. Lett.* **73**, 898 (1994).

²F.O. Schumann, M.E. Buckley, and J.A.C. Bland, *Phys. Rev. B* **50**, 16 424 (1994).

³J. Shen, R. Skomski, M. Klaua, H. Jenniches, S. Sundar Manoharan, and J. Kirschner, *Phys. Rev. B* **56**, 2340 (1997).

⁴H.J. Elmers, J. Hauschild, and U. Gradmann, *Phys. Rev. B* **59**, 3688 (1999).

⁵S. Padovani, I. Chado, F. Scheurer, and J.P. Bucher, *Phys. Rev. B* **59**, 11 887 (1999).

⁶F.M. Leibsle, C.F.J. Flipse, and A.W. Robinson, *Phys. Rev. B* **47**, 15 865 (1993).

⁷F.M. Leibsle, S.S. Dhesi, S.D. Barret, and A.W. Robinson, *Surf. Sci.* **317**, 309 (1994).

⁸T.M. Parker, L.K. Wilson, N.G. Condon, and F.M. Leibsle, *Phys. Rev. B* **56**, 6458 (1997).

⁹Y. Matsumoto and K. Tanaka, *J. Appl. Phys.* **37**, L154 (1998).

¹⁰K. Mukai, Y. Matsumoto, K. Tanaka, and F. Komori, *Surf. Sci.* **450**, 44 (2000).

¹¹S.L. Silva, C.R. Jenkins, S.M. York, and F.M. Leibsle, *Appl. Phys. Lett.* **76**, 1128 (2000).

¹²S.L. Silva and F.M. Leibsle, *Surf. Sci. Lett.* **440**, L835 (1999).

¹³C.M. Schneider, P. Bressler, P. Schuster, J. Kirschner, J.J. de Miguel, and R. Miranda, *Phys. Rev. Lett.* **64**, 1059 (1990).

¹⁴K.D. Lee, T. Iimori, and F. Komori, *Surf. Sci.* **454-456**, 860 (2000).

¹⁵A.K. Schmid, D. Atlan, H. Ito, B. Heinrich, T. Ichinokawa and, J. Kirschner, *Phys. Rev. B* **48**, 2855 (1993).

¹⁶U. Bovensiepen, P. Pouloupoulos, W. Platow, M. Farle, and K. Baberschke, *J. Magn. Magn. Mater.* **192**, L386 (1999).

¹⁷J. Fassbender, R. Allenspach, and U. Durig, *Surf. Sci.* **383**, L742 (1997).

¹⁸L. Néel, *Ann. Geophys. (C.N.R.S.)* **5**, 99 (1949).

¹⁹B. Heinrich, J.F. Cochran, M. Kowalewski, J. Kirschner, *Z. Ce-*

- linski, A.S. Arrott, and K. Myrtle, *Phys. Rev. B* **44**, 9348 (1991).
- ²⁰R. Skomski, D. Sander, J. Shen, and J. Kirschner, *J. Appl. Phys.* **81**, 4710 (1997).
- ²¹S. D'Addato, C. Binns, and P. Finetti, *Surf. Sci.* **442**, 74 (1999).
- ²²A. Berger, U. Linke, and H.P. Oepen, *Phys. Rev. Lett.* **68**, 839 (1992).
- ²³R.K. Kawakami, M.O. Bowen, Hyuk J. Choi, Ernesto J. Escorcia-Aparicio, and Z.Q. Qiu, *Phys. Rev. B* **58**, 5924 (1998).